

## Spiral Defects in Motility Assays: A Measure of Motor Protein Force

L. Bourdieu,<sup>1</sup> T. Duke,<sup>2,\*</sup> M. B. Elowitz,<sup>2</sup> D. A. Winkelmann,<sup>3</sup> S. Leibler,<sup>2</sup> and A. Libchaber<sup>1,4</sup>

<sup>1</sup>The Rockefeller University, 1230 York Avenue, New York, New York 10021

<sup>2</sup>Departments of Physics and of Molecular Biology, Princeton University, Princeton, New Jersey 08544

<sup>3</sup>Department of Pathology, Robert Wood Johnson Medical School, Piscataway, New Jersey 08854

<sup>4</sup>NEC Research Institute, 4 Independence Way, Princeton, New Jersey 08540

(Received 30 January 1995)

In a commonly used motility assay, cytoskeletal filaments are observed as they glide over a surface coated with motor proteins. Defects in the motion frequently interrupt the flow of filaments. Examination of one such defect, in which a filament adopts a spiral form and rotates about a fixed point, provides a simple measure of the force exerted by the motor proteins. We demonstrate the universality of this approach by estimating the elementary forces of both myosin and kinesin.

PACS numbers: 87.15.-v

Molecular motors such as myosin and kinesin play important and multifunctional roles in most higher organisms. Our knowledge of their action is based on experiments which probe their structure, chemistry, and physical properties [1]. The latter experiments, which have concentrated on measurement of velocity and force, are accomplished by *in vitro* motility assays [2–5] and by micromanipulation of individual molecules [6–9]. For example, delicate experiments using optical tweezers [6–8] or microneedles [9] have recently been performed to measure the force produced by single motor enzymes. We show here that an estimate of the average motor force may be obtained in a much more straightforward fashion by studying naturally arising defects in the motion of the associated filaments in motility assays. Despite the microscopic nature and small number of motor proteins interacting with the filaments, these “motility defects” can be analyzed using continuum elasticity theory [10]. We demonstrate this by performing a detailed quantitative study of the actomyosin system and further illustrate the universality of our approach by presenting results for kinesin and microtubules.

The actin motility assays were performed according to a published protocol [11]. Myosin was tethered to a nitrocellulose-coated coverslip via a specific attachment to a monoclonal antibody. Actin labeled with phalloidin-rhodamine was diluted to 3–6 nM with motility buffer, dropped on a slide, and covered with the myosin-coated coverslip. The motion of actin filaments was observed by using fluorescence microscopy. Microtubule motility assays were performed according to a published protocol [12]. Taxol-stabilized microtubules were introduced into a flow cell that had first been coated with casein and then incubated for 3 min with kinesin (70 μg/ml) to saturate the surface. Motility was observed using dark-field microscopy.

When cytoskeletal protein filaments are propelled across a surface coated with motor enzymes, defects in

the motion occasionally disrupt the uniform gliding of the filaments. Most commonly, these occur when a filament gets pinned at its leading tip. This causes it to buckle in the plane of the surface and subsequently to rotate uniformly around the fixed tip (Fig. 1). Precisely what causes the pinning is unknown, although we infer from our observations that it is pointlike [13]. The resulting motility defect, in which a filament adopts a spiral form and whirls around the pinning point, is observed in motility assays of both *F*-actin on myosin [Fig. 1(a)] and microtubules on kinesin [Fig. 1(b)]. Both clockwise and counterclockwise rotations are observed, in the former case with equal probability. Filaments make several revolutions before they break free from the pinning point. The spirals may be characterized by two quantities: their radius and their frequency of rotation. The typical radius is of the order of 1–2 μm for both *F*-actin and microtubules. The rotation frequency at 25 °C is of the order of 0.5 s<sup>-1</sup> for *F*-actin filaments and 0.05 s<sup>-1</sup> for microtubules. Several spirals can be observed simultaneously in the 80 × 60 μm field of view, making possible a statistical study.

To analyze theoretically the dynamics of a filament, we consider a continuum approximation in which the forces applied locally by the motor proteins are replaced by a constant force per unit length, directed along the contour of the filament. This driving force induces both an internal thrust and an elastic bending moment in a pinned filament. Discretizing the filament as a chain of links of unit length with vectors  $\mathbf{u}_i$ , its motion may be examined by numerically solving for the evolution of the position vectors  $\mathbf{r}_i$  of the joints between successive links  $i$  and  $i + 1$ . These obey the Langevin equation

$$\zeta d\mathbf{r}_i/dt = \mathbf{F}_i, \quad (1)$$

where  $\zeta$  is the friction coefficient per unit length and  $\mathbf{F}_i$  is the total force, which comprises four distinct terms:

$$\mathbf{F}_i = (T_i \mathbf{u}_i - T_{i+1} \mathbf{u}_{i+1}) + f(\mathbf{u}_i + \mathbf{u}_{i+1})/2 + k_B T L_p (\mathbf{u}_{i-1} - 3\mathbf{u}_i + 3\mathbf{u}_{i+1} - \mathbf{u}_{i+2}) + \eta_i. \quad (2)$$

The first term describes the effect of the thrust (negative tension)  $T_i$  in each link. The second accounts for the average driving force per unit length  $f$  that the motors exert on the filament. The third term, proportional to the second derivative of the local curvature, is the gradient of the bending energy and varies with persistence length  $L_p$  of the filament (which measures its flexural rigidity  $\kappa_c = k_B T L_p$ ). The final contribution represents thermal noise:  $\eta_i$  is a random force that satisfies the fluctuation-dissipation relation  $\langle \eta_i(t) \eta_j(t') \rangle = 2k_B T \delta_{ij} \delta(t - t')$  in each component. The Langevin equation (1) is numerically integrated with the constraint that the length of each link in the chain remains constant. This constraint determines, in a self-consistent manner, the tension along the chain [14].

The behavior of filaments that encounter a pinning point is investigated by adding to the above description a strong harmonic trapping force that acts only on the terminal point of the filament, restricting its translational

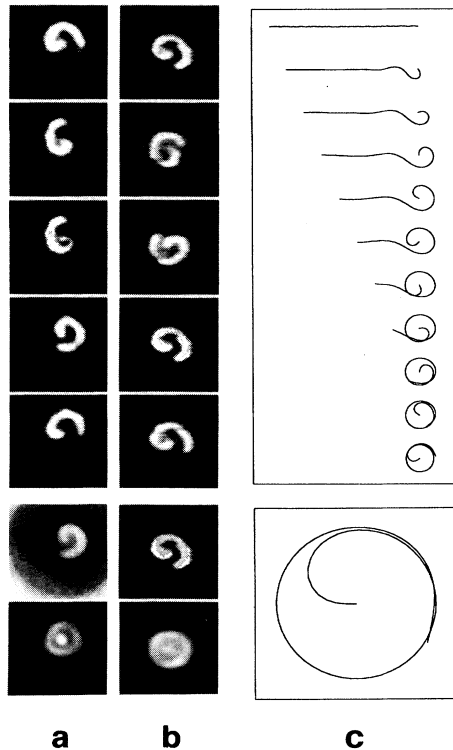


FIG. 1. Time series of the position of a filament pinned at the leading tip and rotating around the fixed point. The size of each image is  $7.5 \mu\text{m}$ . (a) Actin filament on a myosin coated surface. MgATP concentration  $7.5 \text{ mM}$ , temperature  $27.5^\circ\text{C}$ , and time interval  $0.3 \text{ s}$ . (b) Microtubules on a kinesin coated surface. MgATP concentration  $1 \text{ mM}$ , temperature  $25^\circ\text{C}$ , and time interval  $4 \text{ s}$ . (c) Numerical simulation of the formation of a whirling spiral,  $\varepsilon = 5 \times 10^9$ . At the bottom of each column is shown the time average of the filament shape (in the corotating reference frame) and the time average of the filament position (in the fixed reference frame).

motion but permitting free rotation. The filaments buckle [15] and, after a transient period, reach a steady state in which they rotate uniformly about the pinning point while maintaining a constant spiral form [Fig. 1(c)].

A simple scaling argument reveals how the asymptotic radius  $R$  of the spiral varies with the driving force per unit length  $f$ . On the limiting circle, the bending moment is  $M = \kappa_c/R$ . In the steady state, this must be equal to the torque  $\Gamma$  produced by the external forces (the driving force and the friction). Since the radius of the spiral defect is the only relevant length scale,  $\Gamma$  must scale as  $fR^2$ . Thus the condition  $M = \Gamma$  yields the scaling relation

$$R \sim (k_B T L_p / f)^{1/3}. \quad (3)$$

Since on the limiting circle the driving force is exactly opposed by the frictional force, the angular velocity  $\omega$  of rotation is given by  $f = \omega R \zeta$ , so that

$$\omega \sim f^{4/3} / \zeta (k_B T L_p)^{1/3}. \quad (4)$$

In order to make a comparison between the simulated motion and the experimentally observed behavior in different motor systems it is convenient to introduce two dimensionless parameters:  $\rho = R/L_p$  and  $\varepsilon = fL_p^2/(k_B T)$ . Then relation (3) may be written  $\rho = A\varepsilon^{-1/3}$ , where  $A$  is a dimensionless constant.

Figure 2 (inset) shows this dependence between  $\rho$  and  $\varepsilon$  obtained from the numerical simulation. The constant

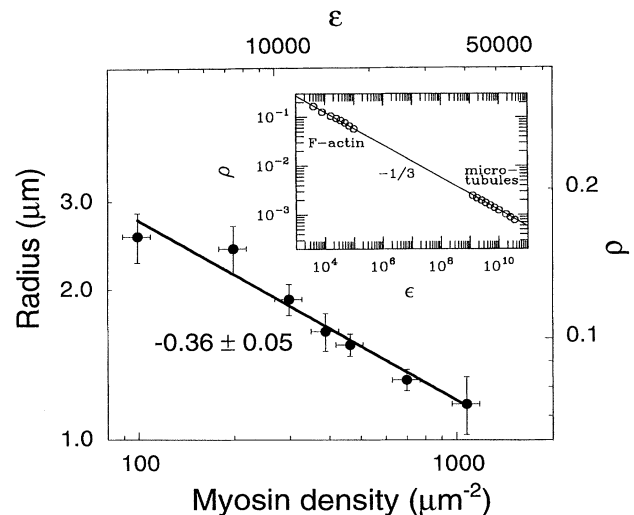


FIG. 2. Radius of the actin filament spiral as a function of the density of myosin. Myosin surface density was changed by varying the volume concentration of myosin drops incubating on an antibody coated coverslip and carefully measured, with 10% accuracy, by radioimmunoassay [11]. The power law fit to the experimental data has exponent  $-0.36 \pm 0.05$ . The corresponding values for  $\varepsilon = fL_p^2/(k_B T)$  and  $\rho = R/L_p$  are indicated for  $L_p = 16 \mu\text{m}$ ,  $wr = 1 \text{ nm}$ , and  $F_0 = 0.6 \text{ pN}$ . Inset: Dependence of  $\rho$  on  $\varepsilon$  obtained by numerical simulation. The straight line is the scaling relation  $\rho = A\varepsilon^{-1/3}$  with  $A = 2.7$ .

of proportionality is determined to be  $A = 2.7$ . The uniformly rotating spiral form is found to be stable for  $\varepsilon > 10^2$ . Below this value, thermal noise disrupts the structure and the direction of rotation frequently reverses. Typical ranges of values  $\varepsilon$  for  $F$ -actin and microtubules are indicated. The distinction between the two systems arises primarily from the widely differing values of the persistence length.

Experimentally, the easiest way to change  $\varepsilon$  for a given motor system is to vary the density of motor proteins on the surface  $\sigma$ , and, thereby, the force per unit length  $f$ . We did this for the actin/myosin assay, where the average density of motors was carefully changed and measured according to a published protocol [11]. As the surface density was decreased from 1000 molecules/ $\mu\text{m}^2$  (a value close to that of saturation of the surface) to 100 molecules/ $\mu\text{m}^2$ , the filaments rotated more slowly and the radius of the spiral increased as shown in Fig. 2. The dependence of the radius on the surface concentration was found to be a power law of exponent  $-0.36 \pm 0.05$ . Fluctuations in the spiral shape were observed to be larger at lower concentrations, a consequence of motor density fluctuations not considered in the theory.

To test the scaling behavior, the relationship between the force per unit length  $f$  and the surface density  $\sigma$  must be established. In a simple model, a filament interacts with motor proteins located in a band of width  $w$ , equal to the characteristic distance over which the enzymes can reach to bind to the filament [3,16]. Let  $F_0$  be the mean force exerted by one motor enzyme during its power stroke and  $r$  (also called the "duty ratio") be the time fraction of the ATPase cycle during which the enzyme is strongly bound to the filament. Then the average distance between two heads that are simultaneously exerting force is  $(wr\sigma)^{-1}$  and the force per unit length is  $f = F_0wr\sigma$  [16]. Equation (3) then predicts

$$R = A(k_B T L_p / F_0 w r)^{1/3} \sigma^{-1/3}. \quad (5)$$

The experimental data are in very good agreement with this scaling. For the actomyosin system, the values  $L_p \approx 16 \mu\text{m}$  [17,18] and  $wr \approx 1-1.5 \text{ nm}$  [19] have been established by independent experiments. Using these values, our data imply that the elementary force of the actin enzyme is  $F_0 \approx 0.5-0.7 \text{ pN}$ . This is comparable with the force per crossbridge measured in muscles [1]. The value is smaller, however, than the force measured in micromanipulation experiments of single myosin molecules [6,9]. We have not performed a similarly accurate measurement of the surface concentration of active kinesin motors, but using reported values for these standards assays [12]  $\sigma = 2000-5000 \text{ molecules}/\mu\text{m}^2$  and  $L_p \approx 5 \text{ nm}$  [18],  $w \approx 20 \text{ nm}$  [20] and  $r \approx 1$  [4,8], the measured spiral radius  $R = 1.3 \mu\text{m}$  implies that the elementary force of the kinesin enzyme is  $F_0 \approx 2-5 \text{ pN}$ . This coincides with most recent estimates obtained by a variety of experimental methods [5,7,8].

In our analysis, we have assumed that the motor force does not depend on the direction of motion of the filament. It is a plausible hypothesis, however, that motors are less effective at exerting force if the filament is moving laterally than if it is gliding along its contour. Theoretically, we investigated the consequences of a motor force which declines as the angle  $\varphi$  between the filament's contour and its direction of motion increases:  $F = F_0 |\cos \varphi|$ . The spiral defect has a slightly different form, but a substantially larger radius: The same scaling law applies but the dimensionless constant increases to  $A = 4.6$ . Our data would then imply an elementary myosin force  $F_0 \approx 3 \text{ pN}$ , which is close to the values obtained by micromanipulation experiments, and a kinesin force  $F_0 \approx 10-25 \text{ pN}$ , considerably larger than all recent estimates. These results and those of the previous paragraph are consistent with the hypothesis that the myosin force depends on the direction of the movement of the filament, but the kinesin force does not.

The influence of temperature on the radius and the angular frequency of the spiral defects has also been examined. Figure 3 shows that the radius is constant within experimental error over the temperature range  $17.5-37.5^\circ\text{C}$ . The frequency of rotation increases as  $\exp(-E_A/k_B T)$ , with an effective activation energy  $E_A = 40k_B T$ . In Eq. (5), the product  $k_B T L_p$  is the flexural rigidity  $\kappa_c$  and is not expected to be strongly dependent on the temperature. Hence, the constancy of the radius implies that the elementary force of the myosin enzyme does not depend appreciably on temperature. The variation of the frequency of rotation implies, from Eq. (3), that the effective friction decreases rapidly with rising temperature. This is consistent with a thermally activated ATPase cycle so that the frequency of application of the kicking force varies as  $\exp(-E_A/k_B T)$ .

In conclusion, it is remarkable that the spiral motility defect, which arises from the interaction of a filament with a small number of motor enzymes, behaves like

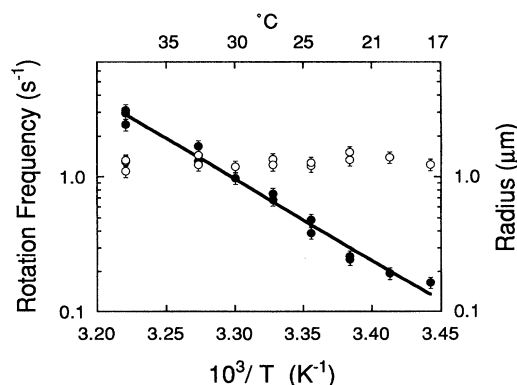


FIG. 3. Temperature dependence of the radius ( $\circ$ ) and angular frequency ( $\bullet$ ) of actin filament spirals. The line is a fit of an exponential to the angular frequency data, with an apparent activation energy of  $40k_B T$ .

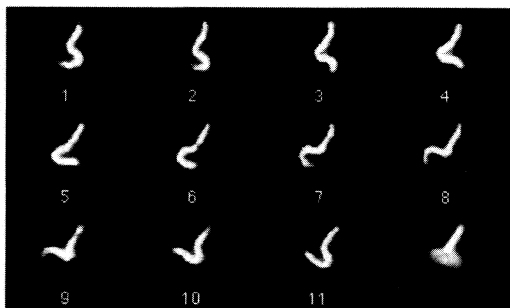


FIG. 4. Time series of the position of an actin filament pinned at the leading tip and developing an undulating motion reminiscent of a flagellum. The last frame is a time average of the series, on which one can see the fixed end segment of the filament. Image size  $10 \mu\text{m}$ , temperature  $27.5^\circ\text{C}$ , and time interval  $0.1 \text{ s}$ .

a macroscopic object with well-defined form and size. At the lowest surface densities examined, only a single myosin molecule (on average) was actively pushing the actin filament at any one instant. Furthermore, we have observed another type of defect which can also be described by the same continuum elastic model. When the pinning is not pointlike, but extends over a line, the filament does not rotate, but undulates like a flagellum (Fig. 4). The same equation of motion describes this defect, but the boundary condition is different—a fixed vector at the end of the filament, rather than a fixed point [21]. As often happens in physics, defects yield more information than can be obtained from a perfect system. In this case, the spiral motility defects provide a ready estimate of the magnitude of the elementary motor force which can be used as a first measurement for newly discovered motor proteins.

This work is supported by NSF Grant No. PHY-9408905. Partial support of NIH (Grant No. GM-50712) and HSFP is also acknowledged. We thank J. Howard for discussions and for providing us with purified kinesin, T. E. Holy for his contribution to the numerical simulation, and A. Ott for this contribution to the actin myosin experimental setup.

\*To whom correspondence should be addressed at the Department of Physics, P.O. Box 708, Princeton, NJ 08544.

[1] C.R. Bagshaw, *Muscle Contraction* (Chapman and Hall, New York, 1993), 2nd ed.

- [2] Y. Harada and T. Yanagida, *Cell. Motil. Cytoskel.* **10**, 71 (1988).
- [3] T. Q. P. Uyeda, S. J. Kron, and J. A. Spudich, *J. Mol. Biol.* **214**, 699 (1990).
- [4] J. Howard, A. J. Hudspeth, and R. D. Vale, *Nature (London)* **342**, 154 (1989).
- [5] A. J. Hunt, F. Gittes, and J. Howard, *Biophys. J.* **67**, 766 (1994).
- [6] J. T. Finer, R. M. Simmons, and J. A. Spudich, *Nature (London)* **368**, 113 (1994).
- [7] S. C. Kuo and M. P. Sheetz, *Science* **260**, 232 (1993).
- [8] K. Svoboda and S. M. Block, *Cell* **77**, 773 (1994).
- [9] A. Ishijima, Y. Harada, H. Kojima, T. Funatsu, H. Higuchi, and T. Yanagida, *Biochem. Biophys. Res. Commun.* **199**, 1057 (1994).
- [10] L. D. Landau and E. M. Lifshitz, *Theory of Elasticity* (Pergamon, New York, 1986), 3rd ed.
- [11] D. A. Winkelmann, L. Bourdieu, A. Ott, F. Kinoshita, and A. Libchaber, *Biophys. J.* (to be published).
- [12] J. Howard, A. J. Hunt, and S. Baek, *Methods Cell Biol.* **39**, 137 (1993).
- [13] One possible microscopic explanation of a pinning point is a defective motor that is permanently in a rigor state.
- [14] J. M. Deutsch, *Science* **240**, 922 (1988).
- [15] Filaments shorter than a critical length simply stop in their tracks when they run into the defect and remain straight apart from small fluctuations caused by thermal noise. Critical buckling length has been used to estimate force in single motor kinesin assays; see F. Gittes, E. Meyhöfer, S. Baek, B. Mickey, and J. Howard, "Nanofabrication and Biosystems", edited by H. C. Hoch, L. W. Jelinski, and H. Craighead (Cambridge Univ. Press, Cambridge, to be published).
- [16] T. Duke, T. E. Holy, and S. Leibler, *Phys. Rev. Lett.* **74**, 330 (1995).
- [17] A. Ott, M. Magnasco, A. Simon, and A. Libchaber, *Phys. Rev. E* **48**, R1642 (1993).
- [18] F. Gittes, B. Mickey, J. Nettleton, and J. Howard, *J. Cell Biol.* **120**, 923 (1993).
- [19] The product  $wr$  has been obtained by fitting  $F$ -actin velocity as a function of filament length at low motor density: Ref. [3] and D. E. Harris and D. M. Warshaw [*J. Biol. Chem.* **268**, 14764 (1993)].
- [20] We estimate  $w$  by assuming that saturation of the surface corresponds to close packing of the enzymes so that  $w \approx \sigma^{-1/2}$ .
- [21] The undulation shown in Fig. 4 is not the asymptotic solution: Long filaments adopt an oscillating form in which they repeatedly trace a figure of eight. We have observed this form in both actin and microtubule assays.

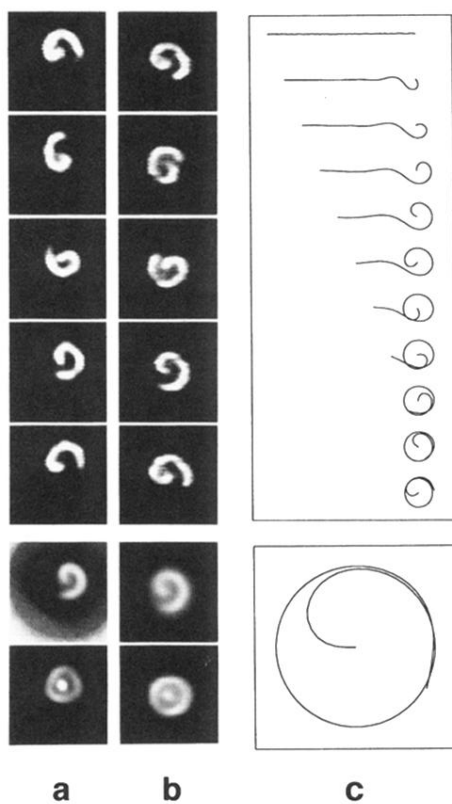


FIG. 1. Time series of the position of a filament pinned at the leading tip and rotating around the fixed point. The size of each image is  $7.5 \mu\text{m}$ . (a) Actin filament on a myosin coated surface. MgATP concentration  $7.5 \text{ mM}$ , temperature  $27.5^\circ\text{C}$ , and time interval  $0.3 \text{ s}$ . (b) Microtubules on a kinesin coated surface. MgATP concentration  $1 \text{ mM}$ , temperature  $25^\circ\text{C}$ , and time interval  $4 \text{ s}$ . (c) Numerical simulation of the formation of a whirling spiral,  $\varepsilon = 5 \times 10^9$ . At the bottom of each column is shown the time average of the filament shape (in the corotating reference frame) and the time average of the filament position (in the fixed reference frame).

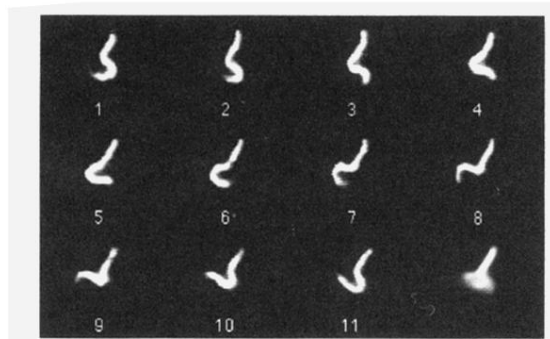


FIG. 4. Time series of the position of an actin filament pinned at the leading tip and developing an undulating motion reminiscent of a flagellum. The last frame is a time average of the series, on which one can see the fixed end segment of the filament. Image size  $10\ \mu\text{m}$ , temperature  $27.5\ ^\circ\text{C}$ , and time interval  $0.1\ \text{s}$ .